**Hydration of a 2D supra-molecular assembly: bitartrate on Cu(110)**

Chenfang Lin, George R. Darling, Matthew Forster, Fiona McBride, Alan Massey and Andrew Hodgson*

*Surface Science Research Centre and Department of Chemistry, University of Liverpool, Liverpool L69 3BX, UK*

**Communicating author* - ahodgson@liverpool.ac.uk

**Abstract**

Hydration layers play a key role in many technical and biological systems, but our understanding of these structures remains very limited. Here we investigate the molecular processes driving hydration of a chiral metal-organic surface, bitartrate on Cu(110), consisting of hydrogen bonded bitartrate rows separated by exposed Cu. Initially water decorates the metal channels, hydrogen bonding to the exposed O ligands that bind bitartrate to Cu, but does not wet the bitartrate rows. At higher temperature water inserts into the structure, breaking existing inter-molecular hydrogen bonds and changing the adsorption site and footprint. Calculations show this process is driven by creation of stable adsorption sites between the carboxylate ligands, allowing hydration of O-Cu ligands within the interior of the structure. This work suggests that hydration of polar metal-adsorbate ligands will be a dominant factor in many systems during surface hydration or self-assembly from solution.

**Introduction**

Solvents play an important role in many chemical reactions, stabilising reactants, products and intermediates differently and so altering reaction rate and chemical selectivity, but our knowledge of their role in heterogeneous processes is remarkably limited [1]. In particular, water is becoming increasingly important as a 'green' solvent to reduce waste, but its role often extends beyond the simple delivery of species to a reaction site, with hydration playing a key role in the formation of solvent-adsorbate complexes that can direct surface chemistry [2-3]. Although techniques to determine chemical identity and adsorbate structure are well developed at solid interfaces, far less is known about the local solvent environment at functional interfaces [4]. In particular, although X-ray and spectroscopic probes may provide evidence for global changes in surface hydration [5-11], detailed molecular scale information is sparse. As a result, despite the key role water plays in many systems [12], insight into its molecular behaviour relies largely on molecular dynamics simulations, with little experimental data to test the detail intrinsic to these models. Understanding the mechanisms by which water re-structures or solvates surface species remains a significant challenge [13-14].

Functionalised surfaces used in technical applications are typically characterised by the combination of strong surface-adsorbate bonds that bind an adsorbate to the solid surface, and weaker lateral interactions that arrange the adsorbate and reactants into a particular structure or pattern on the surface. For example, hydrogen bonding can be used to assemble well-defined 2D supra-molecular surface structures, chemically modifying or patterning a surface to create a particular structure or function. This approach allows us to modify catalytically active surfaces to make them specific to particular adsorbates, or binding geometries, so altering the products formed. An example of this is heterogeneous chiral catalysis, where adsorption of a chiral modifier makes the surface specific to one particular enantiomer, not the other [15]. Since weak, intermolecular hydrogen bonds often play a key role in both assembly of the surface modifier and formation of a surface reaction complex, an understanding of how polar solvents, such as water, modify and hydrate surface structures is important to allow the rational design of new functionalised materials.

One approach to explore surface solvation at the molecular level is to use scanning probe microscopy to examine the initial hydration of simple surface adsorbates, providing an insight into the detailed mechanisms involved in surface hydration. STM has been used to examine the 2D solvation shell formed around several small adsorbates [16-20], but less is known about how extended layers are solvated by water [4, 21-22] and imaging has yet to reveal how hydration proceeds for more complex, non-planar adsorbates. In this study we investigate hydration of a 2D supra-molecular structure, formed by adsorbing tartaric acid onto a metal surface. Tartaric acid is used as a chiral modifier during enantio-selective catalysis and deprotonates to form an extended 2D chiral bitartrate structure on Cu(110) [23]. The bitartrate is strongly bound to Cu by two bidentate carboxylate ligands and ordered into linear structures by weak inter-molecular hydrogen bonds, with a bare metal

channel separating neighbouring bitartrate rows [24]. We show that water initially decorates the metal channels, forming strong hydrogen bonds to the polar O ligands exposed along the edge of the bitartrate rows. Further adsorption forms water clusters along the exposed metal channels, but does not wet the bitartrate rows, which appear hydrophobic, despite the available OH group. At higher temperature water inserts into the bitartrate rows, breaking the hydrogen bonds that stabilize the supra-molecular structure, changing the molecular adsorption site and footprint, and destroying the original chiral structure. DFT calculations show this process is driven by creation of stable water binding sites between the polar carboxylate ligands, allowing hydration of O ligands within the interior of the supra-molecular structure. Since many important systems rely on highly-polar ligands to stabilize surface adsorbates, we expect that hydration of the metal-ligand sites will be of general importance in understanding how surface-adsorbate systems respond to the presence of water.

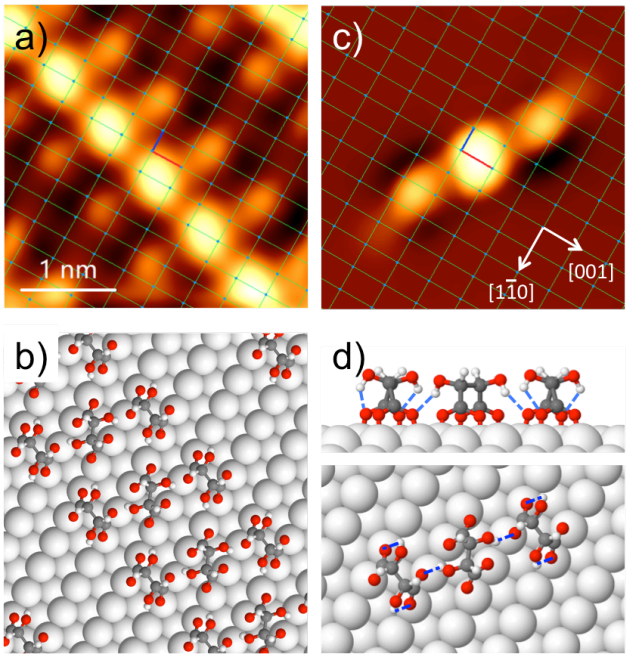


Figure 1. STM images showing (R, R) bitartrate adsorbed on Cu(110). a) STM image showing detail of the extended 2D chiral (9 0, 1 2) bitartrate structure, with the surface Cu atoms indicated by the rectangular net. b) calculated structure for bitartrate on Cu(110). c) STM showing an isolated $R_{ec}O_bR_{ec}$ bitartrate trimer formed at low coverage and d) its structure, with the hydrogen bonds indicated by dashed blue lines. Images recorded at 80 K, -0.4 V, 100 pA and -0.51 V, 66 pA respectively.

**Results and Discussion**

Tartaric acid de-protonates the carboxylate groups at ~400 K on Cu(110), forming an ordered chiral bitartrate phase whose behaviour has been investigated in detail [23-28]. Bitartrate binds to Cu via the carboxylate O atoms, forming bidentate ligands that allow it to bridge across adjacent close packed Cu rows [23, 27], as shown in Figure 1. Under usual experimental conditions the bitartrate assembles into extended trimer chains, separated by a channel of bare Cu, forming the 2D chiral structure shown in Figure 1a,b. By recording STM images of low coverage regions, where aggregation into extended 2D structures is inhibited by the finite diffusion length, we are also able to identify isolated bitartrate trimers on the Cu(110) terraces, as shown in Fig. 1c. The appearance of isolated trimers, in preference to individual bitartrate molecules, indicates that the trimer is the thermodynamically stable unit, consistent with DFT structure calculations that find the trimer is held together by inter-molecular H-bonds, with weak dispersion and through-surface interactions assembling the trimers into rows to form the 2D structure [24].

Both the isolated bitartrate trimer and the extended chain structure appear similar in STM, with the central molecule having a higher contrast than its two neighbours. Comparison of STM images with electronic structure calculations [24] shows that the trimer has a hydrogen bonded structure in which the central bitartrate bonds to the surface with an oblique ($O_b$) footprint, while the two outer molecules adopt a rectangular ($R_{ec}$) footprint, bonded directly across neighbouring Cu rows as shown in Fig. 1b,d. Whereas the outer molecules are stabilised in the $R_{ec}$ footprint by intra-molecular hydrogen bonds between OH and its adjacent O ligand [27], these hydrogen bonds are broken in the central molecule, which instead adopts an oblique footprint to allow OH to hydrogen bond to the neighbouring molecules [24]. Distorting an isolated bitartrate into the $O_b$ footprint is unfavourable, but is repaid by formation of strong inter-molecular hydrogen bonds in the $R_{ec}O_bR_{ec}$ trimer. Strain in the metal surface, caused by bonding to carboxylate [26], prevents the bitartrate rows stacking next to each other and stabilises the open structure (Figure 1a). Despite the high binding energy of bitartrate to Cu, the reliance on hydrogen bonds to stabilise the super-structure suggests this phase may be sensitive to the presence of water that disrupts its hydrogen bonding. Moreover, the contrast of bitartrate in STM images is sensitive to changes in its local configuration, providing a way to explore the effect of co-adsorbed water on the bitartrate structure during hydration, even when the water itself may not be directly visible by STM.

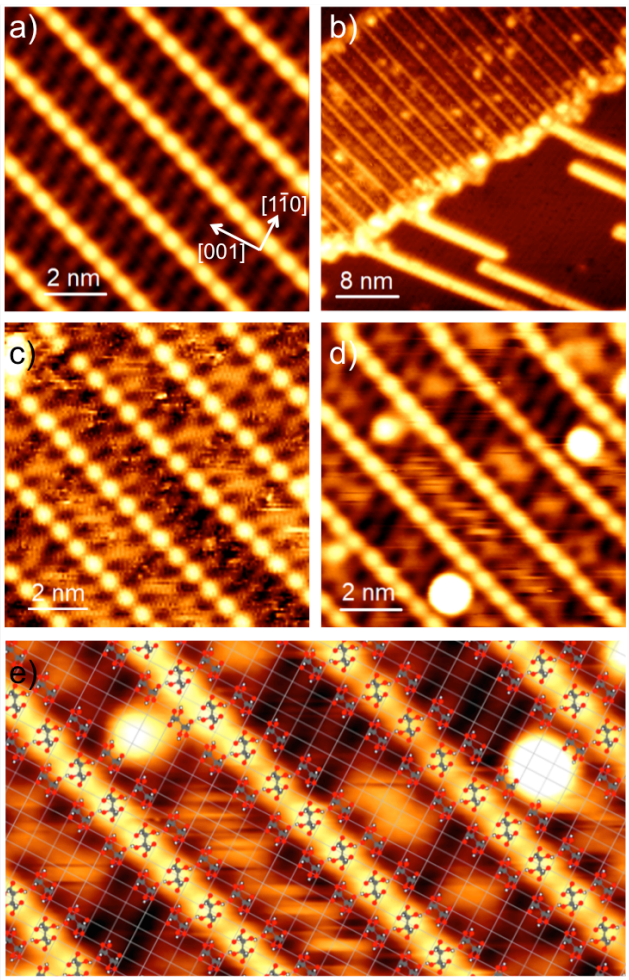


Figure 2. STM images comparing a bitartrate surface (a) before and (b-d) after water adsorption at 80 K. (b) large scale image for 0.11 ML water adsorbed on a bitartrate island. (c) detail of (b) showing water forming mobile features and diffuse structures in the Cu channels between bitartrate rows. Increasing the water coverage to 0.25 ML (d) results in large amorphous clusters appearing along the Cu channels above low contrast zigzag structures. (e) Schematic showing the surface Cu net, indicated by the grid, and the location of bitartrate in (d) relative to the features caused by water in the Cu channels. The images were recorded at (a, b) -0.1 V, 10 pA, (c) -0.21 V, 20 pA and (d) -0.21 V, 100 pA respectively.

The effect of exposing a bitartrate island to water at low temperature is shown in Fig. 2. Depositing a small amount of water results in the appearance of water pentamer chains on the Cu(110) terraces [29], nucleated from the bitartrate island edges. The bitartrate islands themselves remain intact, (Fig. 2b), but water clusters appear as bright features at the edge of the islands and along the Cu channels between the trimer rows. These bright clusters show no particular structure and often appear diffuse, indicating they are amorphous. At higher resolution the Cu channels also show low contrast zigzag structures and mobile features (Fig. 2c) that are easily displaced by the STM tip. The mobile features reduce as the coverage is increased, Fig. 2d, with faint zigzag features apparent in parts of the Cu channel, alongside larger water clusters. The bitartrate itself appears unchanged by

water adsorption and is shown superimposed on the STM image in Fig. 2e. The features caused by water adsorption remain confined to the Cu channels, rather than restructuring or decorating the top of the bitartrate rows, and are attributed to weakly bound or low coordinate water that can easily be displaced within the Cu channel by the STM tip. Increasing the coverage further results in the water clusters growing larger and more numerous, decorating the Cu channels until they obscure the outer bitartrate molecules from view to leave only the central bitartrate rows visible between the clusters (see for example Figs. 3g and S1 for further details). The overall behaviour at low temperature is that the Cu channels act as hydrophilic sites and the bitartrate rows as hydrophobic, despite the presence of OH groups on bitartrate that might stabilise water above the bitartrate chain.

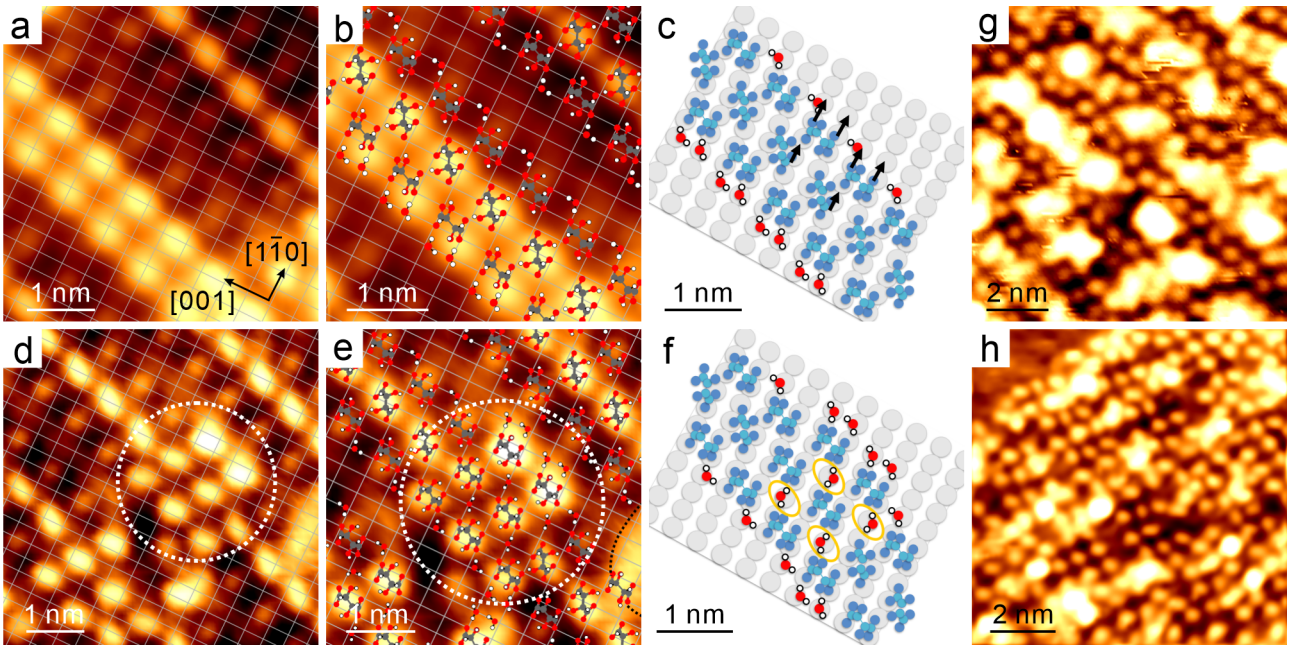


Figure 3. STM images showing the effect of water on bitartrate as the temperature is increased. a, d) STM images showing detail of the bitartrate structure in the presence of 0.1 ML water at 120 K. The grid shows the underlying Cu surface net. a) shows a row of bitartrate along the edge of a trimer row increasing in contrast, while (b) shows water locally expanding the trimer row and disrupting the original bitartrate structure (circled). b, c) and (e, f) show schematics, based on DFT calculations described in the text, indicating water-bitartrate arrangements consistent with images (a) and (b). The solid arrows in (c) show the movement required to change the two bitartrate trimers (c) into the structure shown in (d-f). In (g) increasing the water coverage (*ca.* 0.3 ML) at 120 K forms water clusters in the Cu channels, while (h) shows the complete loss of long range order of bitartrate after the surface is annealed to 150 K to remove weakly bound water clusters. The imaging conditions are (a, b, e) 0.4 V, 100 pA and (f) 0.34 V, 100 pA.

Increasing the surface temperature increases the mobility of both water and bitartrate, changing the adsorption behaviour, as shown in Fig. 3. The zigzag water structures seen at 80 K (Fig. 2d) disappear from the Cu channels, implying these structures are metastable. Water surrounding the

edge of bitartrate islands orders into recognisable H-bonding networks similar to those seen on clean Cu(110) [30-31]. Apart from the appearance of large water clusters in the Cu channels as the coverage is increased (Fig. 3g), STM no longer images any other water directly, but its presence can be inferred from changes to the bitartrate structure. We observe two distinct types of change to the bitartrate layer. The first, most common change observed at low temperature (T≤120 K), is an increase in contrast of bitartrate molecules along the edge of the trimer rows, forming a series of bright features down one or both sides of the bitartrate row, as shown in Fig. 3a (see also Fig. S1). The increase in contrast is associated with a slight shift (less than half the Cu spacing) in the intensity maximum of these features along the bitartrate row, as shown in Fig. 3b. Formation of the bright rows maintains the overall bitartrate structure, with no increase in trimer width, and occurs occasionally even at 80 K.

The second type of modification to bitartrate is more significant, involving local restructuring of the trimer chains. At these sites the outer bitartrate molecules increase in intensity and some of the bitartrate groups change their adsorption footprint and site. An example is shown circled in Fig. 3d, where a pair of bitartrate trimers increase in contrast and are displaced relative to the underlying Cu grid. The central molecule of the trimer changes appearance, aligning more along <001>, and displaces by half a unit along <1-10>, consistent with bitartrate moving from an oblique footprint across two Cu unit cells to a rectangular adsorption site in a single Cu unit cell, as illustrated in Fig. 3e,f. Simultaneously, the outer molecule displaces in the same direction and increases in contrast. This results in an increased width for the trimer chain, with bitartrate sitting in the adsorption sites expected for a $R_{ec}R_{ec}R_{ec}$ trimer, creating bare Cu sites within the structure that are not bonded to bitartrate (highlighted yellow in Fig. 3f). This rearrangement often occurs to several bitartrate trimers in a local group, suggesting the process is concerted, with bitartrate rearrangement creating space within the chains that allows water into the structure, encouraging further disruption of neighbouring sites. As the water dose is increased, Fig. 3g, large water clusters form along the Cu channels, obscuring many of the outer bitartrate groups. Nevertheless, the bitartrate along the centre of the original trimer chains remain clear of water clusters, with individual molecules displaced irregularly either side of the original site, similar to bitartrate in Fig. 3d. Heating the surface to 150 K or above (Fig. 3h) desorbs water that is stabilised only by weak water-water H-bonds [32], removing the water clusters seen at lower temperature and leaving only strongly bonded water. The increased mobility of water and bitartrate at 150 K results in the complete disappearance of the original bitartrate chains. The surface now consists of bitartrate adsorbed across the surface in a disordered fashion, Fig. 3h, and the original bitartrate structure can only be recovered by annealing the surface to the original preparation temperature (350 - 400 K) to drive off the remaining water and re-order bitartrate. The progression from local changes to the bitartrate chains at low temperature (80 K) to complete dissolution at higher temperature (150 K) indicates that water progressively disrupts the

tartaric acid structure, solvating the bitartrate units to form a disordered, hydrated 2D bitartrate-water phase.

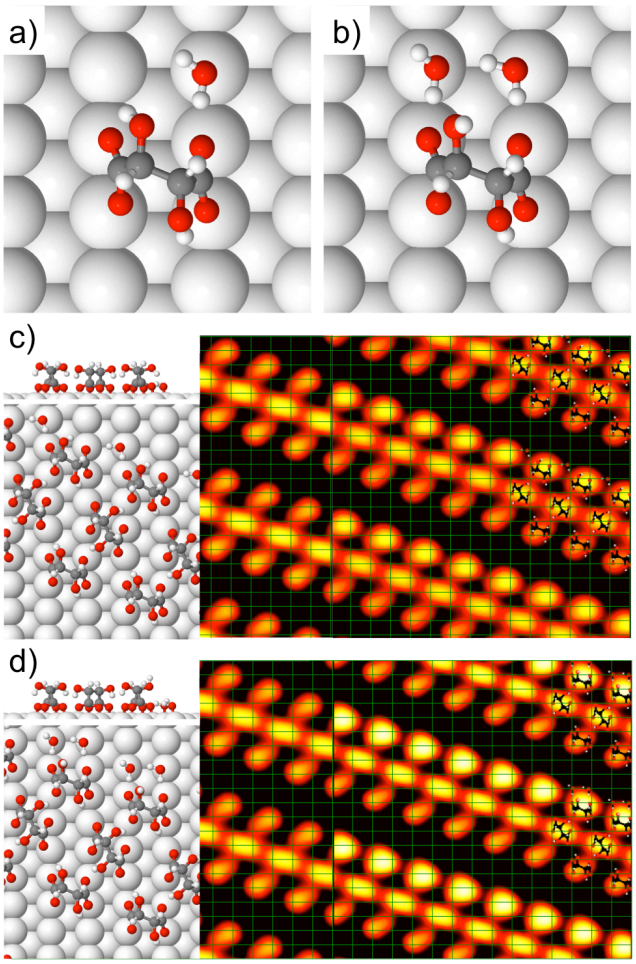


Figure 4. Electronic structure calculations showing the minimum energy adsorption geometry of one or two water molecules next to bitartrate, with a binding energy of (a-d) 0.957, 1.04, 1.089 and 1.04 eV/water respectively. a, b) show water next to bitartrate monomer with the rectangular footprint and (c, d) the water structure next to bitartrate rows. The background in (c, d) compares a simulation of the STM images (0.3 V bias) showing bitartrate alone (LHS) or with water (RHS). The grid indicates the position of the Cu atoms. The contrast of bitartrate in (d) increases as 2 waters bind to the O ligands, breaking the internal H-bond and shifting the maximum contrast towards the uncoordinated OH group (see Fig 3a-c).

In order to understand the mechanism by which bitartrate is solvated we performed extensive DFT calculations to explore how water binds, what causes some molecules at the outside of the trimer chains to increase in contrast and why water breaks apart the bitartrate structure. A summary of the calculated structures, their binding energy and STM simulations are provided in the SI. The calculations show that water prefers to bind next to bitartrate, adsorbing flat atop a neighbouring Cu to form a hydrogen bond to the O ligand, as shown in Fig. 4a. The adsorption geometry is similar to

water on the bare surface, but the binding energy for water is 0.466 eV greater than for an isolated water on Cu and 0.195 eV greater than for the pentamer chains formed on bare Cu terraces [29]. The four Cu sites immediately adjacent to the O ligands all offer a similar binding energy, but when water donates to the O ligand adjacent to the OH group, the internal H-bond breaks and reforms to the opposite carboxylate ligand, distorting the bitartrate structure. The presence of two H donors alongside the bitartrate causes the internal H-bond to break entirely, as shown in Figs. 4b and S6, leaving the OH group pointing away from the surface. Despite breaking the internal bitartrate hydrogen bond, water adsorption has negligible effect on the relative stability of the $R_{ec}$ versus $O_b$ footprints (see Fig. S4-S6).

Water adsorption onto the extended bitartrate structure follows a similar pattern, water preferentially decorating the edge of the trimer rows as it forms a hydrogen bond to the O ligands (Fig. S7). Figure 4c shows the most stable structure we found with water decorating one edge of the trimer row. Water binds between two bitartrate molecules, forming a hydrogen bond to an O ligand on each molecule. Formation of the new water H-bond causes bitartrate to reorient its internal H-bond so the OH group binds to the opposite O ligand in a 6 member ring. Water shows a low contrast in STM and simulations (Figs. 4c) show that the water molecules are invisible next to bitartrate and cannot be directly imaged in STM. When additional water is adsorbed onto this structure it binds flat in the Cu channel, forming H-bond networks that show a low contrast in STM (see Fig. S8 and SI for more details). These structures are metastable, being less stable than structures where water and bitartrate is allowed to fully restructure, but will form kinetically at low temperature as water decorates the stable hydration structure. This behaviour reproduces the experimental observation that a low contrast water network forms in the Cu channel at 80 K (Fig. 2d) but disappears when the surface is annealed to 120 K (Fig. 3a,d) and water and bitartrate are able to relax into more stable configurations.

When a second water is added alongside bitartrate, water forms a dimer next to the O ligands, as shown in Fig. 4d and S7. In this case the water H-bonds to the O ligands cause bitartrate to completely break the internal hydrogen bond, so that the OH group now becomes free to rotate. STM simulations (Fig. 4d) show a large increase in contrast of the bitartrate near the free OH, consistent with the shift in intensity maximum towards that end of the molecule observed experimentally (Fig. 3b). Decoration of the edge of the bitartrate chains requires no displacement of the adsorbate and only limited local relaxation of the structure as water bonds to the O ligands and breaks the internal hydrogen bond. As a result this process is expected to have a low activation barrier and is observed occasionally even at 80 K, but occurs more frequently above 100 K (Fig. S1). Experimentally we find that the contrast increase in bitartrate often occurs for a number of neighbouring molecules, as shown in Fig. 3a, suggesting an ordered chain of water forms along side the bitartrate row, causing the same relaxation at a series of sites. The DFT calculations support the

idea that the local coordination around bitartrate determines if the internal OH group simply relaxes (Fig. 4c), or breaks (Fig. 4d) causing the bitartrate to 'light up' in STM. These results indicate that hydration of the Cu-O ligands along the edge of the Cu channels occurs even at 80 K, and represents the first stage of bitartrate hydration.

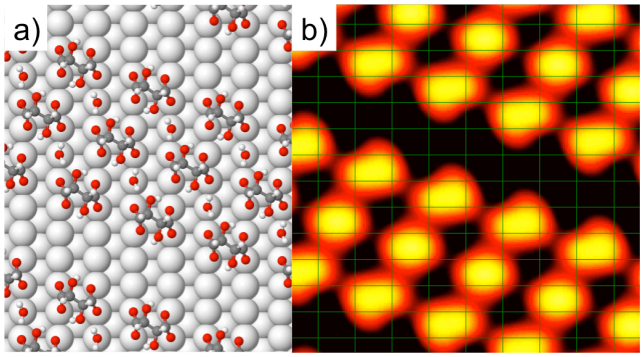


Figure 5. Calculated structure showing the most stable arrangement found for two water molecules adsorbed per bitartrate trimer with a binding energy of 1.235 eV/water. a) shows the resulting $R_{ec}R_{ec}R_{ec}$ trimers with water adsorbed on the exposed Cu site. b) empty states STM simulation for 0.3 V bias with the grid showing the Cu surface net.

In order to explore why water causes expansion of the bitartrate structure at higher temperatures (Fig. 3d,h) we compared water adsorption on the original bitartrate arrangement with structures obtained by displacing bitartrate into a different site or footprint. Water adsorption on top of the original ($R_{ec}O_bR_{ec}$) bitartrate structure is extremely unfavourable, but restructuring the chains by changing the adsorption footprint, or by displacing bitartrate into neighbouring sites, creates open chains with new adsorption sites that strongly bind water (Fig. S9). Displacing bitartrate laterally creates the ($R_{ec}R_{ec}R_{ec}$) trimer observed in Fig. 3d, opening up vacant Cu sites between the bitartrate groups, as shown schematically in Fig. 3e,f. Water can adsorb at these vacant Cu sites as shown in Fig. 5, hydrating the Cu-O ligands in the interior of the chains and stabilising the ($R_{ec}R_{ec}R_{ec}$) configuration. This structure is the most stable arrangement we found with 2 waters per trimer, and is more stable than structures where water decorates the edge of the bitartrate rows. Water adsorbs atop the vacant Cu site, forming H-bonds to the two neighbouring O-Cu ligands. Although the new structure has sacrificed the inter-molecular H-bond found in the original ($R_{ec}O_bR_{ec}$) trimer, this is compensated by the additional hydration energy. However, unlike relaxation of the internal H-bonds at the edge of a bitartrate row, restructuring a trimer requires the O ligands to displace along the close packed Cu row. This process is activated, occurring only occasionally at 80 K but becoming more common as the temperature is increased towards 120 K where there is sufficient thermal energy to allow bitartrate to change adsorption site. The formation of water H-bonds to the O ligands in the ($R_{ec}R_{ec}R_{ec}$) trimer cause the internal bitartrate H-bonds to reorient towards O on the opposite end of the molecule, twisting the C skeleton and increasing the contrast in STM, Fig. 5b, similar to

the experimental behaviour shown in Fig 3d. At higher temperatures, where mobility is greater, further restructuring can provide additional Cu adsorption sites, allowing more water into the rows and eventually causing the complete breakup of the bitartrate structure shown in Figure 3h. In support of this idea, several different trimer arrangements that allow water into the structure are more stable than structures with water confined to the outside edge alone (see SI Fig. S9).

The idea that hydration of O ligands within the interior of the structure drives bitartrate restructuring gains further support from the observation of similar changes for isolated bitartrate trimers. In this case it is possible to directly resolve the water network formed around the trimer, see Fig. 6 and S3. Bitartrate trimers are immediately recognisable as three bright features, surrounded by a low contrast 2D water network in STM images. The water/OH hydrogen bond structures can be assigned based on previous work [29-36], defining the Cu surface net and allowing the trimer to be assigned to a particular configuration. Whereas $R_{ec}O_bR_{ec}$ trimers are found exclusively on the clean surface, and may persist up to ca. 120 K during hydration (see SI Fig. S3), at higher temperatures hydration creates open $R_{ec}R_{ec}R_{ec}$ trimers, shown in Fig. 6. Just as for the extended 2D structure, restructuring the trimer allows water greater access to the Cu-O ligands between the groups, with two new O ligands becoming accessible to water in the more open $R_{ec}R_{ec}R_{ec}$ structure (indicated by the dark blue O atoms shown schematically in Fig. 6b).

Our results show that hydration of chemisorbed bitartrate is driven by the high binding energy of water at metal sites immediately next to carboxylate O ligands. The original bitartrate structure has accessible O-Cu ligands available along the edge of the bitartrate rows, and water decorates these sites at low temperature. Local relaxation of the internal bitartrate H-bonds occurs in response to the new water H-bonds, with multiple water H-bonds breaking the internal bitartrate H-bond even at low temperature. In contrast, water adsorbed on top of the bitartrate structure, where it can form H-bonds to the OH group and O ligands, loses the favourable Cu-water interaction and is unstable. The original trimer rows don't have any vacant Cu sites within the structure where water could bind, but increasing the temperature allows water to penetrate into the bitartrate rows and displace bitartrate to create stable Cu adsorption sites between the O ligands. Heating to 150 K causes the trimers to separate, fully hydrating the Cu-O ligands and completely disrupting the original bitartrate structure, a process that occurs some 200 K below the temperature required to re-order bitartrate alone. By replacing the inter-molecular H-bonds that stabilise bitartrate trimers with H-bonds to water, water adsorption destroys the long-range chiral structure. We conclude that any chiral activity of surface bitartrate in the presence of water can only arise from a direct local interaction with bitartrate.

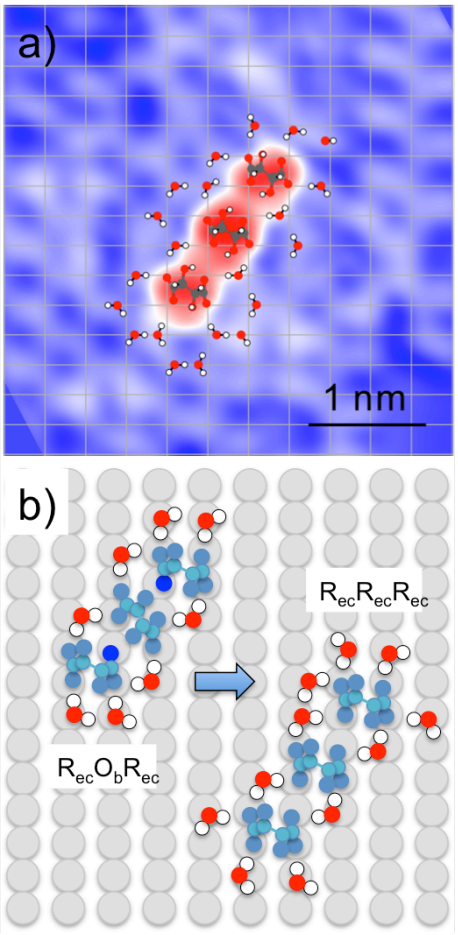


Fig. 6. a) STM image showing a single $R_{ec}R_{ec}R_{ec}$ trimer surrounded by a water/OH network after annealing at 150 K to order water (-0.4 V, 100 pA). The trimer images with a high contrast (red) while the water network appears as a low contrast (white) network above the Cu (blue), with the Cu lattice sites indicated by the grid. The occupied water adsorption sites immediately around the bitartrate trimer are indicated schematically, although the specific proton orientations are unknown. b) Schematic comparing the number of water H-bonding sites around the original $R_{ec}O_bR_{ec}$ hydrogen bonded trimer (left) to the relaxed $R_{ec}R_{ec}R_{ec}$ trimer (right). Oxygen ligand sites that are inaccessible to water in the original $R_{ec}O_bR_{ec}$ trimer are highlighted in bright blue, showing the creation of additional water adsorption sites around the $R_{ec}R_{ec}R_{ec}$ trimer.

Many supported adsorbate systems used in technical applications, such as surface protection or functionalization, rely on their wetting behaviour to different materials for their operation [37-39], creating great interest in how water is structured within and immediately above the surface film [13, 40-42]. Surface functionalization is often achieved by patterning the surface with an organic functional group, mediated by specific adsorption of the self-assembled layer via a polar ligand. Examples of such systems include SAMs based on S, O or N containing ligands, but experimental characterisation of these overlayers remains limited [43-44]. Recently new neutron reflection studies have revealed that Au thiol SAMs, probably the most intensively investigated system, show an unanticipated degree of water penetration into the interface, with between two and 6 water per

adsorbed ligand [45], directly influencing the behaviour of the SAM. The behaviour displayed for the bitartrate system investigated here indicates that hydration of polar surface-adsorbate ligands is expected to occur by adsorption at nearest neighbour surface sites, suggesting a general mechanism for water adsorption on hydrophilic surfaces protected by an adsorbate film. A better understanding of the atomic arrangement of these interfaces will provide a way to anticipate the effect of this water and the consequences for surface packing and the growth or disruption of self-assembled films

**Conclusion**

We have shown that hydration of a chiral, supramolecular assembly is driven by hydration of the O ligands that are responsible for binding the adsorbate to the metal surface. Initially the accessible O-Cu ligands are decorated by water but, as the coverage increases, water disrupts the dense adsorbate chains, breaking the intra-molecular H-bonds to allow water in to hydrate all of the O ligands. This process is progressive, with local restructuring allowing further water into the structure. Despite having an OH group that can form H-bonds to water, the bitartrate itself appears hydrophobic, with the OH groups playing a limited role in hydration. Since many supported adsorbate systems rely on highly polar ligands to chemisorb on the surface, we anticipate that hydration of polar surface-adsorbate ligands will play a key role in the hydration behaviour of many technically important surfaces.

**Methods**

**Experimental**. The Cu(110) surface was prepared by argon ion sputtering at 500 eV, followed by annealing to 800 K, yielding an average terrace size of *ca.* 800 Å. Further details have been given previously [30]. R,R tartaric acid (99%) was obtained from Sigma Aldrich and used without purification. The adsorbate was deposited from a solid sample held in a resistively heated glass tube, separated from the main vacuum chamber by a gate valve and differentially pumped by a turbomolecular pump [24]. The tartaric acid was outgassed at *ca.* 340 K and then heated to *ca.* 370 K to sublime onto the copper crystal. After deposition the Cu sample was heated to 350 K to de-protonate the acid and desorb the hydrogen. The ordering of the bitartrate phase and its structure was confirmed by LEED and STM.

STM images were recorded in an ultra high vacuum STM (Createc STM/AFM at 77 K) operated in constant current mode with an electrochemically etched tungsten tip. Images were acquired in constant current mode, with bias voltages quoted relative to the sample, so that positive voltages correspond to electrons tunnelling into the surface (empty state images). Water was adsorbed on the bitartrate structures in situ at 80 K using a directional doser. The surface was then annealed to the desired temperature using a diode heater, before cooling to 80 K in order to image the surface. Heating the surface from 80 K to 150 K to desorb water clusters required ca. 2 hours. STM images

were processed using WSxM [46]. Preliminary experiments to characterise water adsorption in this system were carried out using a Specs 150 Aarhus STM at 100 K, with low current LEED and TPD to characterise water adsorption using methods described earlier [47-48]. Figures S1 to S3 show supporting STM images of water adsorption on the 2D bitartrate structure and around an isolated trimer. Assignment of bitartrate to different adsorption footprints ($R_{ec}$ or $O_b$) is made using the location of the bitartrate relative to the Cu surface net. The Cu atom locations are established either from the Cu location in STM (isolated trimers or small bitartrate islands), the known structure of the bitartrate phase (large bitartrate islands at T≤120 K) or from the OH/water network around an isolated trimer (e.g. Fig. 6). It is not possible to establish the bitartrate adsorption site and footprint when no ordered structure is present, for example when bitartrate is fully hydrated and disordered at 150 K (Fig. 4h).

**Computational details.** Total energy calculations were carried out for trial structures using VASP [49-50] with the optB86b-vdW exchange-correlation functional [51-52]. The optB86b-vdW functional includes van der Waals interactions, which are known to be important in stabilizing surface adsorption relative to cluster formation [53-54], and has a similar performance to other vdW functionals for systems where physisorption is important [55]. Water adsorption on a single bitartrate was modeled with a (5x4) supercell in a 5 layer slab, with the bottom two layers fixed, using a 7x6x1 k-point mesh (see Fig. S3-S5). The extended 2D structure in the (9 0, 1 2) (R,R) unit cell used a 4x12x1 k-point set, see Figs. S6-S8. Valence electron-core interactions were included using the projector augmented wave method [56-57], with a plane wave cutoff energy of 400 eV and including dipole corrections perpendicular to the surface. All water adsorption energies are quoted in eV per molecule, calculated relative to the original bitartrate covered Cu(110) surface and water in the gas phase. Adsorption energies are not corrected for vibrational effects. Figures S3-S8 show supporting calculations referred to in the text. Simulation of the STM images were calculated using the Tersoff-Hamann approximation in the implementation by Lorente and Persson [58-59].

**Supporting Information**

Supporting Information is available for this paper and includes additional STM images, electronic structure calculations and binding energies for all the structures discussed in the text.

**Acknowledgements**

This work was supported by the EPSRC via grant EP/K039687/1 and used the UK Materials and Molecular Modelling Hub for computational resources, via our membership of the UK's HEC Materials Chemistry Consortium funded by EPSRC (EP/L000202, EP/R029431**)**, which is partially funded by EPSRC (EP/P020194). Work was also undertaken on Barkla, part of the High Performance Computing facilities at the University of Liverpool, UK.

**References**


1. Li, G. N.; Wang, B.; Resasco, D. E., Water-Mediated Heterogeneously Catalyzed Reactions. *Acs Catalysis* **2020,** *10* (2), 1294-1309.

2. Zhao, Z.; Bababrik, R.; Xue, W. H.; Li, Y. P.; Briggs, N. M.; Nguyen, D. T.; Nguyen, U.; Crossley, S. P.; Wang, S. W.; Wang, B.; Resasco, D. E., Solvent-mediated charge separation drives alternative hydrogenation path of furanics in liquid water. *Nature Catalysis* **2019,** *2* (5), 431-436.

3. Bodenschatz, C. J.; Xie, T. J.; Zhang, X. H.; Getman, R. B., Insights into how the aqueous environment influences the kinetics and mechanisms of heterogeneously-catalyzed COH* and CH3OH* dehydrogenation reactions on Pt(111). *Phys. Chem. Chem. Phys.* **2019,** *21* (19), 9895-9904.

4. Lucht, K.; Trosien, I.; Sander, W.; Morgenstern, K., Imaging the Solvation of a One-Dimensional Solid on the Molecular Scale. *Ang. Chem.* **2018,** *57* (50), 16334-16338.

5. Wu, C. H.; Pascal, T. A.; Baskin, A.; Wang, H.; Fang, H.-T.; Liu, Y.-S.; Lu, Y.-H.; Guo, J.; Prendergast, D.; Salmeron, M. B., The molecular scale structure of electrode-electrolyte interfaces: the case of platinum in aqueous sulfuric acid. *J. Am Chem. Soc.* **2018,** *140* (47), 16237-16244.

6. Li, C. Y.; Le, J. B.; Wang, Y. H.; Chen, S.; Yang, Z. L.; Li, J. F.; Cheng, J.; Tian, Z. Q., In situ probing electrified interfacial water structures at atomically flat surfaces. *Nature Mat.* **2019,** *18* (7), 697.

7. Cyran, J. D.; Donovan, M. A.; Vollmer, D.; Brigiano, F. S.; Pezzotti, S.; Galimberti, D. R.; Gaigeot, M. P.; Bonn, M.; Backus, E. H. G., Molecular hydrophobicity at a macroscopically hydrophilic surface. *Proc. Nat. Acad. Sci.* **2019,** *116* (5), 1520-1525.

8. Mirabella, F.; Zaki, E.; Ivars-Barcelo, F.; Li, X. K.; Paier, J.; Sauer, J.; Shaikhutdinov, S.; Freund, H. J., Cooperative Formation of Long-Range Ordering in Water Ad-layers on Fe3O4(111) Surfaces. *Ang. Chem.* **2018,** *57* (5), 1409-1413.

9. Schaefer, J.; Backus, E. H. G.; Bonn, M., Evidence for auto-catalytic mineral dissolution from surface-specific vibrational spectroscopy. *Nature Communications* **2018,** *9*, 3316.

10. Esser, A.; Forbert, H.; Sebastiani, F.; Schwaab, G.; Havenith, M.; Marx, D., Hydrophilic Solvation Dominates the Terahertz Fingerprint of Amino Acids in Water. *J. Phys. Chem. B* **2018,** *122* (4), 1453-1459.

11. Shavorskiy, A.; Aksoy, F.; Grass, M. E.; Liu, Z.; Bluhm, H.; Held, G., A Step toward the Wet Surface Chemistry of Glycine and Alanine on Cu{110}: Destabilization and Decomposition in the Presence of Near-Ambient Water Vapor. *J. Am. Chem. Soc.* **2011,** *133* (17), 6659.

12. Saleheen, M.; Heyden, A., Liquid-Phase Modeling in Heterogeneous Catalysis. *Acs Catalysis* **2018,** *8* (3), 2188-2194.

13. Li, S. S.; Wu, L.; Zhang, X. F.; Jiang, X. E., The Structure of Water Bonded to Phosphate Groups at the Electrified Zwitterionic Phospholipid Membranes/Aqueous Interface. *Ang. Chem.* **2020,** *59* (16), 6627-6630.

14. Magnussen, O. M.; Gross, A., Toward an Atomic-Scale Understanding of Electrochemical Interface Structure and Dynamics. *J. Am. Chem. Soc.* **2019,** *141* (12), 4777-4790.
15. Mallat, T.; Orglmeister, E.; Baiker, A., Asymmetric catalysis at chiral metal surfaces. *Chem. Rev.* **2007,** *107* (11), 4863-4890.
16. Koshida, H.; Hatta, S.; Okuyama, H.; Shiotari, A.; Sugimoto, Y.; Aruga, T., Water-NO Complex Formation and Chain Growth on Cu(111). *J. Phys. Chem. C* **2018,** *122* (16), 8894-8900.
17. Henzl, J.; Boom, K.; Morgenstern, K., Influence of water on supra-molecular assembly of 4,4 '-dihydroxy azobenzene on Ag(111). *J. Chem. Phys.* **2015,** *142* (10), 101920.
18. Lechner, B. A. J.; Kim, Y.; Feibelman, P. J.; Henkelman, G.; Kang, H.; Salmeron, M., Solvation and Reaction of Ammonia in Molecularly Thin Water Films. *J. Phys. Chem. C* **2015,** *119* (40), 23052-23058.
19. Lucht, K.; Loose, D.; Ruschmeier, M.; Strotkotter, V.; Dyker, G.; Morgenstern, K., Hydrophilicity and Microsolvation of an Organic Molecule Resolved on the Sub-molecular Level by Scanning Tunneling Microscopy. *Ang. Chem.* **2018,** *57* (5), 1266-1270.
20. Zhang, C.; Xie, L.; Ding, Y. Q.; Xu, W., Scission and stitching of adenine structures by water molecules. *Chemical Communications* **2018,** *54* (7), 771-774.
21. Tan, S. J.; Feng, H.; Zheng, Q. J.; Cui, X. F.; Zhao, J.; Luo, Y.; Yang, J. L.; Wang, B.; Hou, J. G., Interfacial Hydrogen-Bonding Dynamics in Surface-Facilitated Dehydrogenation of Water on TiO2(110). *J. Am. Chem. Soc.* **2020,** *142* (2), 826-834.
22. Peng, J. B.; Guo, J.; Ma, R. Z.; Meng, X. Z.; Jiang, Y., Atomic-scale imaging of the dissolution of NaCl islands by water at low temperature. *J. Phys. Cond. Mat.* **2017,** *29* (10), 104001.
23. Lorenzo, M. O.; Baddeley, C. J.; Muryn, C.; Raval, R., Extended surface chirality from supramolecular assemblies of adsorbed chiral molecules. *Nature* **2000,** *404* (6776), 376-379.
24. Darling, G. R.; Forster, M.; Lin, C.; Liu, N.; Raval, R.; Hodgson, A., Chiral segregation driven by a dynamical response of the adsorption footprint to the local adsorption environment: bitartrate on Cu(110). *Phys. Chem. Chem. Phys.* **2017,** *19* (11), 7617-7623.
25. Lawton, T. J.; Pushkarev, V.; Wei, D.; Lucci, F. R.; Sholl, D. S.; Gellman, A. J.; Sykes, E. C. H., Long Range Chiral Imprinting of Cu(110) by Tartaric Acid. *J. Phys. Chem. C* **2013,** *117* (43), 22290-22297.
26. Hermse, C. G. M.; van Bavel, A. P.; Jansen, A. P. J.; Barbosa, L.; Sautet, P.; van Santen, R. A., Formation of chiral domains for tartaric acid on Cu(110): A combined DFT and kinetic Monte Carlo study. *J. Phys. Chem. B* **2004,** *108* (30), 11035-11043.
27. Barbosa, L.; Sautet, P., Stability of chiral domains produced by adsorption of tartaric acid isomers on the Cu(110) surface: A periodic density functional theory study. *J. Am. Chem. Soc.* **2001,** *123* (27), 6639-6648.
28. Lorenzo, M. O.; Haq, S.; Bertrams, T.; Murray, P.; Raval, R.; Baddeley, C. J., Creating chiral surfaces for enantioselective heterogeneous catalysis: R,R-Tartaric acid on Cu(110). *J. Phys. Chem. B* **1999,** *103* (48), 10661-10669.

29. Carrasco, J.; Michaelides, A.; Forster, M.; Raval, R.; Hodgson, A., A Novel One Dimensional Ice Structure Built from Pentagons. *Nature Mat.* **2009,** *8*, 427.
30. Forster, M.; Raval, R.; Carrasco, J.; Michaelides, A.; Hodgson, A., Water-hydroxyl phases on an open metal surface: breaking the ice rules. *Chem. Sci.* **2012,** *3*, 93.
31. Forster, M.; Raval, R.; Hodgson, A.; Carrasco, J.; Michaelides, A., c(2 x 2) water-hydroxyl layer on Cu(110): a wetting layer stabilized by Bjerrum defects. *Phys. Rev. Lett.* **2011,** *106*, 046103.
32. Schiros, T.; Haq, S.; Ogasawara, H.; Takahashi, O.; Öström, H.; Andersson, K.; Pettersson, L. G. M.; Hodgson, A.; Nilsson, A., Structure of water adsorbed on the open Cu(110) surface: H-up, H-down, or both? *Chem. Phys. Lett.* **2006,** *429*, 415.
33. Yamada, T.; Tamamori, S.; Okuyama, H.; Aruga, T., Anisotropic water chain growth on Cu(110) observed with scanning tunneling microscopy. *Phys. Rev. Lett.* **2006,** *96* (3), 036105.
34. Kumagai, T.; Okuyama, H.; Hatta, S.; Aruga, T.; Hamada, I., Water clusters on Cu(110): Chain versus cyclic structures. *J. Chem. Phys.* **2011,** *134* (2), 024703.
35. Shiotari, A.; Sugimoto, Y., Ultrahigh-resolution imaging of water networks by atomic force microscopy. *Nature Communications* **2017,** *8*, 14313.
36. Hamada, I.; Kumagai, T.; Shiotari, A.; Okuyama, H.; Hatta, S.; Aruga, T., Nature of hydrogen bonding in hydroxyl groups on a metal surface. *Phys. Rev. B* **2012,** *86* (7), 075432.
37. Zhang, J. L.; Gu, C. D.; Tu, J. P., Robust Slippery Coating with Superior Corrosion Resistance and Anti-Icing Performance for AZ31B Mg Alloy Protection. *Acs Applied Materials & Interfaces* **2017,** *9* (12), 11247-11257.
38. Wang, Z. X.; Elimelech, M.; Lin, S. H., Environmental Applications of Interfacial Materials with Special Wettability. *Environmental Science & Technology* **2016,** *50* (5), 2132-2150.
39. Falde, E. J.; Yohe, S. T.; Colson, Y. L.; Grinstaff, M. W., Superhydrophobic materials for biomedical applications. *Biomaterials* **2016,** *104*, 87-103.
40. Pawlowska, N. M.; Fritzsche, H.; Blaszykowski, C.; Sheikh, S.; Vezvaie, M.; Thompson, M., Probing the Hydration of Ultrathin Antifouling Organosilane Adlayers using Neutron Reflectometry. *Langmuir* **2014,** *30* (5), 1199-1203.
41. Guo, P.; Tu, Y. S.; Yang, J. R.; Wang, C. L.; Sheng, N.; Fang, H. P., Water-COOH Composite Structure with Enhanced Hydrophobicity Formed by Water Molecules Embedded into Carboxyl-Terminated Self-Assembled Monolayers. *Phys. Rev. Lett.* **2015,** *115* (18), 186101.
42. Fies, W. A.; First, J. T.; Dugger, J. W.; Doucet, M.; Browning, J. F.; Webb, L. J., Quantifying the Extent of Hydration of a Surface-Bound Peptide Using Neutron Reflectometry. *Langmuir* **2020,** *36* (2), 637-649.
43. Liu, P. X.; Qin, R. X.; Fu, G.; Zheng, N. F., Surface Coordination Chemistry of Metal Nanomaterials. *J. Am. Chem. Soc.* **2017,** *139* (6), 2122-2131.
44. Casalini, S.; Bortolotti, C. A.; Leonardi, F.; Biscarini, F., Self-assembled monolayers in organic electronics. *Chemical Society Reviews* **2017,** *46* (1), 40-71.

45. Fies, W. A.; Dugger, J. W.; Dick, J. E.; Wilder, L. M.; Browning, K. L.; Doucet, M.; Browning, J. F.; Webb, L. J., Direct Measurement of Water Permeation in Submerged Alkyl Thiol Self-Assembled Monolayers on Gold Surfaces Revealed by Neutron Reflectometry. *Langmuir* **2019,** *35* (16), 5647-5662.

46. Horcas, I.; Fernandez, R.; Gomez-Rodriguez, J. M.; Colchero, J.; Gomez-Herrero, J.; Baro, A. M., WSXM: A software for scanning probe microscopy and a tool for nanotechnology. *Rev. Sci. Inst.* **2007,** *78* (1), 013705.

47. McBride, F.; Hodgson, A., The reactivity of water and OH on Pt-Ni(111) films. *Phys. Chem. Chem. Phys.* **2018,** *20* (24), 16743-16748.

48. Massey, A.; McBride, F.; Darling, G. R.; Nakamura, M.; Hodgson, A., The role of lattice parameter in water adsorption and wetting of a solid surface. *Phys. Chem. Chem. Phys.* **2014,** *16* (43), 24018-24025.

49. Kresse, G.; Furthmuller, J., Efficient iterative schemes for ab initio total-energy calculations using a plane-wave basis set. *Phys. Rev. B* **1996,** *54* (16), 11169-11186.

50. Kresse, G.; Hafner, J., Abinitio Molecular-Dynamics for Liquid-Metals. *Phys. Rev. B* **1993,** *47* (1), 558-561.

51. Klimes, J.; Bowler, D. R.; Michaelides, A., Chemical accuracy for the van der Waals density functional. *J. Phys. Cond. Mat.* **2010,** *22* (2), 022201.

52. Klimes, J.; Bowler, D. R.; Michaelides, A., Van der Waals density functionals applied to solids. *Phys. Rev. B* **2011,** *83* (19), 195131.

53. Carrasco, J.; Santra, B.; Klimes, J.; Michaelides, A., To wet or not to wet? Dispersion forces tip the balance for water ice on metals. *Phys. Rev. Lett.* **2011,** *106*, 026101.

54. Gillan, M. J.; Alfe, D.; Michaelides, A., Perspective: How good is DFT for water? *J. Chem. Phys.* **2016,** *144* (13), 130901.

55. Hanke, F.; Dyer, M. S.; Bjork, J.; Persson, M., Structure and stability of weakly chemisorbed ethene adsorbed on low-index Cu surfaces: performance of density functionals with van der Waals interactions. *J. Phys. Cond. Mat.* **2012,** *24* (42), 424217.

56. Blöchl, P. E., Projector augmented-wave method. *Phys. Rev. B* **1994,** *50*, 17953-17979.

57. Kresse, G.; Joubert, D., From ultrasoft pseudopotentials to the projector augmented-wave method. *Phys. Rev. B* **1999,** *59*, 1758-1775.

58. Tersoff, J.; Hamann, D. R., Theory And Application For The Scanning Tunneling Microscope. *Phys. Rev. Lett.* **1983,** *50* (25), 1998-2001.

59. Lorente, N.; Persson, M., Theoretical aspects of tunneling-current-induced bond excitation and breaking at surfaces. *Faraday Discuss.* **2000,** *117*, 277-290.

TOC